

Structure and cluster formation in granular media

S LUDING

Particle Technology, DelftChemTech, TU Delft, Julianalaan 136, 2628 BL Delft,
The Netherlands

E-mail: s.luding@tnw.tudelft.nl

Abstract. The two most important phenomena at the basis of granular media are excluded volume and dissipation. The former is captured by the hard sphere model and is responsible for, e.g., crystallization, the latter leads to interesting structures like clusters in non-equilibrium dynamical, freely cooling states. The freely cooling system is examined concerning the energy decay and the cluster evolution in time. Corrections for crystallization and multi-particle contacts are provided, which become more and more important with increasing density.

Keywords. Clustering; freely cooling granular gas; event-driven simulation; global equation of state; TC model; multi-particle contacts.

PACS Nos 45.70.Qj; 45.70.-n; 64.60.Ak

1. Introduction

Granular media and their interesting behavior have caught a lot of attention in the last decades, see [1–4]. One reason is their ability to form a hybrid state between a fluid and a solid: Energy input leads to a reduction of the density due to more collisions and increasing pressure, so that the material can flow, i.e. it becomes ‘fluid’. On the other hand, in the absence of energy input, granular materials become denser, i.e. they ‘solidify’ due to dissipation. The same co-existence of fluid and solid states also happens without energy input in freely cooling systems, where extremely dilute regions co-exist with very high-density, solid clusters. The basic idea of clustering is that in an initially homogeneous, freely cooling granular gas, fluctuations in density, velocity, and temperature cause a position-dependent energy loss. This causes locally inhomogeneous dissipation; pressure and energy drop inhomogeneously and material moves from ‘hot’ to ‘cold’ regions, leading to even stronger dissipation in the denser, cold regions. This phenomenon is examined numerically mainly by means of hard sphere molecular dynamics simulations [5–9]. Only recently, the hydrodynamic theory [10,11] for the early stages [12] of the onset of clustering is accompanied by numerical solutions of the hydrodynamic equations [9,13].

In the dense regime, the particles contact more frequently so that multi-particle contacts are more likely and – *not* directly related to multi-particle collisions – crystallization occurs above a specific density. All these make granular media an interesting multi-particle system with a rich phenomenology, as detailed in the following section.

2. Simulation details

A granular gas can be idealized as an ensemble of hard spheres in which the energy loss that accompanies the collision of macroscopic particles is modeled with a single coefficient of restitution. In the simplest case the particles are identical in size and mass and there are no inter-particle forces between collisions.

Details about initial and boundary conditions are given in §2.1. The microscopic dynamics of the motion and the collision of the particles are discussed in §2.2 and the simulation method is explained in §2.3. Section 2.4 deals with the inelastic collapse, a problematic artefact of the hard sphere model with dissipation.

2.1 Initial and boundary conditions

The simulation volume consists of a box with equal side length and periodic boundary conditions in two dimensions (2D) and three dimensions (3D). An initial state with random particle positions and velocities is prepared in the following way: The particles first sit on a regular lattice and get a random velocity with a total momentum of zero. Then the simulation is started without dissipation ($r = 1$) and runs for about 10^2 collisions per particle so that the system becomes homogeneous and the velocity distribution approaches a Maxwellian. This state is now used as initial configuration for the dissipative simulations.

2.2 Microscopic dynamics

The particles are idealized as hard spheres; this means that collisions take zero time and involve only two particles. Between collisions no forces act upon the particles and they move at constant velocity. Conservation of momentum leads to the collision rule

$$\vec{v}'_{1/2} = \vec{v}_{1/2} \mp \frac{1+r}{2} (\hat{\mathbf{k}} \cdot (\vec{v}_1 - \vec{v}_2)) \hat{\mathbf{k}}, \quad (1)$$

where a prime indicates the velocities \vec{v} after the collision and $\hat{\mathbf{k}}$ is a unit vector pointing along the line of centers from particle 1 to particle 2. The relative tangential velocity does not change during a collision and the relative normal velocity changes its sign and is reduced by a factor $1 - r$, with the restitution coefficient r . So at each collision, the kinetic energy of the relative velocity's normal component is reduced by the factor $\lambda = 1 - r^2$. The elastic limit $r = 1$ implies no dissipation ($\lambda = 0$), while $r < 1$ implies $\lambda > 0$.

2.3 Event-driven molecular dynamics

The simulation of hard spheres can be handled efficiently with event-driven molecular dynamics [14,15]. The collisions are the events which have to be treated by the algorithm. Between these collisions the particles move on trivial trajectories and so the algorithm can easily compute the point of time t_{12} of the next collision of two particles 1 and 2 as $t_{12} = t_0 + s_{12}/v_{12}^2$, with $s_{12} = -\vec{r}_{12} \cdot \vec{v}_{12} - \sqrt{(\vec{r}_{12} \cdot \vec{v}_{12})^2 - (r_{12}^2 - (2a)^2)v_{12}^2}$, where $\vec{v}_{12} = \vec{v}_2(t_0) - \vec{v}_1(t_0)$ and $\vec{r}_{12} = \vec{r}_2(t_0) - \vec{r}_1(t_0)$ are the relative velocities and positions of the particles at time t_0 , and a is the radius of a particle.

The algorithm processes the events one after the other. After a collision the positions and velocities of the two involved particles are updated, the state of all other particles remains unchanged. For the two involved particles new events are calculated and the next future event is stored in the event priority queue for both particles. The next event is obtained from the priority queue, the new positions and velocities after the collision for the collision partners are updated, and so on. Neighborhood search is enhanced with standard linked cell methods [16], where the cell change of a particle is treated as a new event type. The details of the algorithm can be found in [14,15,17].

2.4 Avoiding the inelastic collapse with the TC model

Our model makes use of hard spheres with an infinitely stiff interaction potential. As a consequence, the contact duration is implicitly zero, matching well the corresponding assumption of instantaneous contacts used for the kinetic theory [18,19]. However, due to this artificial simplification, ED algorithms run into problems when the time between events t_n gets too small: In dense systems with strong dissipation, t_n may even tend to zero – the dramatic consequence is the ‘inelastic collapse’. This singularity is unphysical, of course, and a major drawback for numerical simulations, too. But it has been shown that one can circumvent this artefact of the dissipative hard sphere model with the so-called TC model in the following way [20]: If two consecutive collisions of a particle happen within a small time t_c , dissipation is switched off for the second collision. The time t_c can be seen as a typical duration of a contact, and allows for the definition of the dimensionless ratio

$$\tau_c = t_c/t_n. \quad (2)$$

The effect of t_c on the simulation results is negligible for large r and small t_c (for a more detailed discussion see [6,20,21]).

There exist other deterministic and random models which prevent inelastic collapse (see [20] for a discussion and [21] for the kinetic theory solution for the cut-off type of models). Since almost all of them lack a solid theoretical background and physical motivation, we apply the TC model in the following.

3. Numerical experiments

The simulation is started from a homogeneous system, prepared as described in §2.1. Depending on the dissipation λ , the density ν , and the number N of particles, the system remains in the homogeneous cooling regime for some time (or for very low λ , ν , and N even forever) until clustering starts and the system becomes inhomogeneous. First, we focus on the homogeneous cooling state and discuss the regime where multi-particle collisions are likely.

3.1 Kinetic energy and collision frequency

Dissipative collisions lead to a decay of the kinetic energy and the collision frequency (see figure 1). Besides that, these figures show three different regimes:

- The homogenous cooling state (HCS), when no clusters have formed yet at short times, can be described by a mean-field kinetic theory (see [22] and references therein). The decay of the kinetic energy E is governed by the equation

$$E := K(\tau)/K(0) = (1 + \tau)^{-2}, \quad (3)$$

with the scaled time $\tau = \lambda t/[2Dt_E(0)]$. D is the dimension of the system and $t_E(0)$ is the initial Enskog collision rate at time $t = 0$, where

$$t_E = \sqrt{\pi}a/[2^{D-1}D\nu g_D(\nu)\sqrt{T/m}]. \quad (4)$$

Here, $T = 2K/(DN)$ is the so-called ‘granular temperature’ (i.e. twice the kinetic energy per particle per degree of freedom), a the particle radius, ν is the volume fraction, and g_D is the contact probability. In 2D, $g_2(\nu) = (1 - 7\nu/16)/(1 - \nu)^2$ and in 3D $g_3(\nu) = (1 - \nu/2)/(1 - \nu)^3$. The evolution of the collision frequency per particle with time is given by $f_c(\tau) = t_E^{-1}(0)\sqrt{K(\tau)/K(0)}$, valid for $D = 2$ and $D = 3$.

- In the cluster growth regime, the decays of energy and collision rate decrease and deviate from the HCS laws. The collision frequency strongly fluctuates and the decay of the kinetic energy slows down. Note that the average collision frequency may even increase. The deviation from eq. (3) occurs earlier and is more dramatic for larger dissipation λ , i.e. smaller r . However, the cluster growth regime is characterized by an energy decay $E \sim \tau^{-1}$, independently of r and D [8]. In contrast, the qualitative behavior of the collision frequency clearly depends on r . The deviation from the HCS is more distinct for larger dissipation and larger systems.
- Finally, in the saturation regime, when the largest cluster in the population has reached system size, the cooling resembles – in some cases – the homogeneous cooling state in so far that $E(\tau) \propto \tau^{-2}$ and $f_c(\tau) \propto \tau^{-1}$, even if these quantities show large fluctuations due to the enormous changes of both energy and collision rate during cluster–cluster interactions.

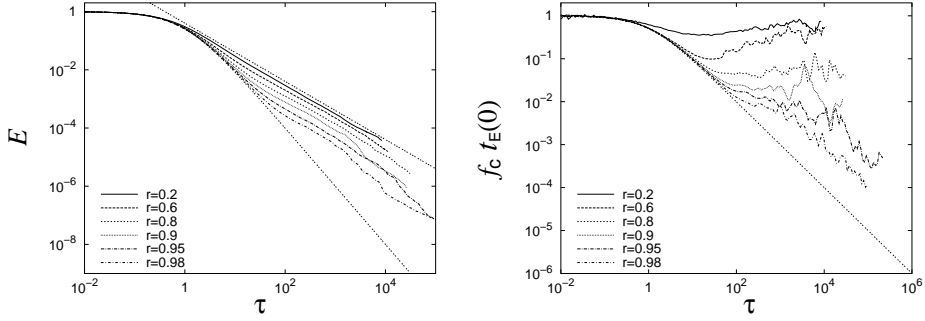


Figure 1. Decay of the kinetic energy E (left) and the collision frequency f_c (right) plotted against scaled time τ in a 2D system with $N = 316^2 = 99856$ particles, volume fraction $\nu = 0.25$, and different restitution coefficients r . The lines give eq. (3) and τ^{-1} .

3.2 Dense HCS with multi-particle contacts

In dense systems two phenomena can become important:

First, above a certain density ($\nu \approx 0.7$ in 2D and $\nu \approx 0.56$ in 3D), systems of monodisperse spheres crystallize. Crystallization leads to order and thus to an enhanced mean free path between collisions. Therefore, the term $\nu g_D(\nu)$ in eq. (4) has to be corrected via a so-called ‘global equation of state’ [23]. This issue was discussed extensively for 2D systems [23,24], so that we do not go into more details here, we rather refer to [25].

Second, for very high density – corresponding to very small mean free path – there is a finite chance in assemblies of (real) soft particles, that multi-particle contacts occur. Therefore, in real systems, the artefact of an inelastic collapse is avoided. (Because every collision takes a finite time, an infinite collision rate is impossible.) The TC model can be seen as a means to allow for multi-particle collisions in dense systems [20,21,26,27], where it is known that multi-particle contacts reduce dissipation [28]. In the case of a homogeneous cooling system (HCS), one can explicitly compute the corrected, scaled cooling rate (right hand side) in the energy balance equation

$$dE/d\tau = -2I(E, t_c), \tag{5}$$

with the dimensionless time $\tau = \lambda t/[6t_E(0)]$ for 3D systems, with $T = 2K/(3N)$. In these units, the energy dissipation rate I is a function of the dimensionless energy $E = K/K(0)$ with the kinetic energy K , and the cut-off time t_c . In this representation, the restitution coefficient is hidden in the rescaled time via λ , so that inelastic hard sphere simulations with different r scale on the same master-curve. When the classical dissipation rate $E^{3/2}$ [18] is extracted from I , so that $I(E, t_c) = J(E, t_c)E^{3/2}$, one has the correction-function $J \rightarrow 1$ for $t_c \rightarrow 0$. The deviation from the classical HCS is [21]:

$$J(E, t_c) = \exp(\Psi(x)) \tag{6}$$

with the series expansion $\Psi(x) = -1.268x + 0.01682x^2 - 0.0005783x^3 + \mathcal{O}(x^4)$ in the collision integral, with $x = \sqrt{\pi}t_c t_E^{-1}(0)\sqrt{E} = \sqrt{\pi}\tau_c(0)\sqrt{E} = \sqrt{\pi}\tau_c$ [21]. This is close to the result $\Psi_{\text{LM}} = -2x/\sqrt{\pi}$, proposed by Luding and McNamara, based on probabilistic mean-field arguments [20] – Ψ_{LM} thus neglects non-linear terms and underestimates the linear part.

Given the differential equation (5) and the correction due to multi-particle contacts from eq. (6), it is possible to obtain the solution numerically, and to compare it to the classical $E_\tau := (1 + \tau)^{-2}$ solution. Simulation results are compared to the theory in figure 2 (left). The agreement between simulations and theory is almost perfect in the examined range of t_c values. Only when deviations from homogeneity are evidenced, one expects disagreement between simulation and theory. The fixed cut-off time t_c has no effect when the time between collisions is very large ($t_E \gg t_c$), but strongly reduces dissipation when the collisions occur with high frequency $t_E^{-1} \gtrsim t_c^{-1}$. Thus, in the homogeneous cooling state, there is a strong effect initially, and if t_c is large, but the long-time behavior tends towards the classical decay $E \rightarrow E_\tau \propto \tau^{-2}$.

The final check if the ED results obtained using the TC model are reasonable is to compare them to MD simulations (see figure 2 (right) and ref. [29] for details concerning the MD simulation). Open and solid symbols correspond to soft and hard sphere simulations respectively. The qualitative behavior (the deviation from the classical HCS solution) is identical: The energy decay is delayed due to multi-particle collisions, but later the classical solution is recovered. A quantitative comparison shows that the deviation of E from E_τ is larger for ED than for MD, given that the same t_c is used. This weaker dissipation can be understood from the strict rule used for ED: Dissipation is inactive if any particle had a contact already.

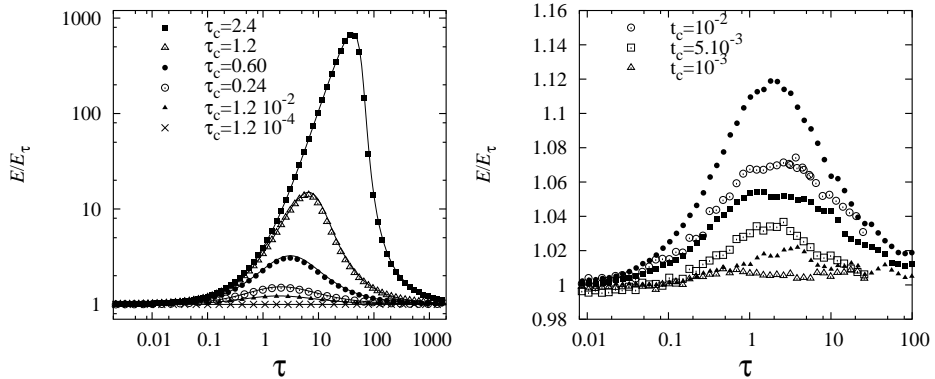


Figure 2. (Left) Deviation from the HCS, i.e. rescaled energy E/E_τ , with $E_\tau = (1 + \tau)^{-2}$. The data are plotted against τ for simulations with different $\tau_c(0) = t_c/t_E(0)$ as given in the figure, with $r = 0.99$, and $N = 8000$. Symbols are ED simulation results, the solid line results from the third-order correction (see text for details). (Right) E/E_τ plotted against τ for simulations with $r = 0.99$ and $N = 2197$. Solid symbols are ED simulations, open symbols are MD (soft particle simulations) with three different t_c as given in the figure.

The disagreement between ED and MD is systematic and should disappear if about 30 per cent smaller t_c value is used for ED. The disagreement is also plausible, since the TC model disregards all dissipation for multi-particle contacts, while the soft particles still dissipate energy – even though much less – in the case of multi-particle contacts [28].

3.3 Cluster growth

After several collisions per particle, the first deviations from the HCS occur (if the dissipation and the density are large enough). In the following, exemplary snapshots are shown and the evolution of the cluster size distribution is examined.

The first picture in figure 3 is taken shortly after the initially homogeneous cooling regime, whereas the next two pictures show the later stages of the cluster growth and the saturation regime. The particles are colored spots, where the green/red areas in the cluster centers correspond to particles with collision rate $t_n^{-1} \geq 50 \text{ s}^{-1}$. This is much smaller than the critical collision rate $t_c^{-1} = 10^5 \text{ s}^{-1}$, so that only a very small number of particles will be affected by the TC model, in the center of the clusters.

The energy loss of the particles first leads to a reduced separation velocity after collision and eventually to the formation of clusters. Note that already for very short times, deviations from the homogeneous regime become evident when one examines the short-range pair-distance probability distribution function. But the definition of a cluster suffers from the fact that it takes a huge (possibly infinite) number of collisions until the particles could stay in permanent contact with each other [6]. So we use the following definition: Two particles belong to the same cluster, if their distance is smaller than $s = 0.1$ particle diameters. The choice of s is arbitrary and a different choice leads to quantitatively different results; the key informations do not depend on s .

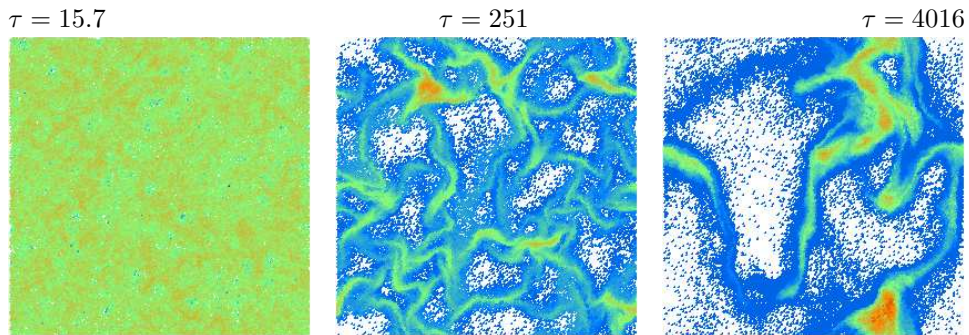


Figure 3. ED simulation with $N = 99856$ particles in a system of size $L = 560$, volume fraction $\nu = 0.25$, restitution coefficient $r = 0.9$, and critical collision frequency $t_c^{-1} = 10^5 \text{ s}^{-1}$. The collision frequency is color-coded: red, green and blue correspond to collision rates $t_n^{-1} \approx 250 \text{ s}^{-1}$, 50 s^{-1} and 10 s^{-1} , respectively.

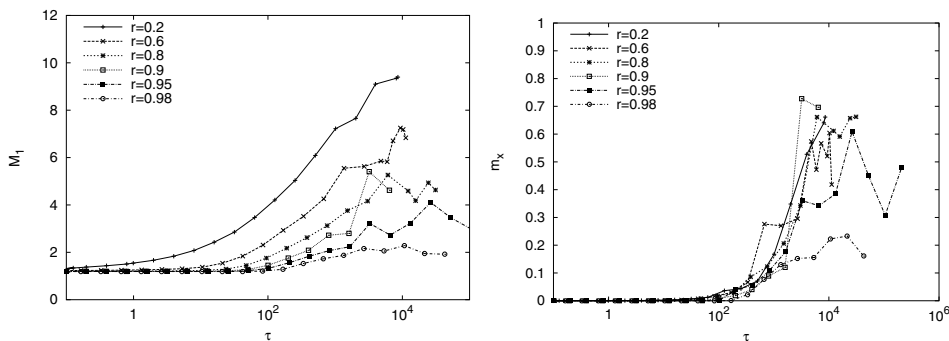


Figure 4. Growth of the first moment of the cluster size distribution M_1 (left) and of the fraction of the largest cluster m_x (right), plotted against scaled time τ in a 2D system with $N = 99856$ particles, volume fraction $\nu = 0.25$, and different restitution coefficients r .

The moments of the cluster size distribution M_k are defined as

$$M_k := \frac{1}{n_c} \sum_i i^k n_i, \quad (7)$$

where n_c denotes the total number of clusters and n_i the number of clusters of size i . In many cases there are a lot of small clusters and one large cluster of size n_x , which contains a macroscopic fraction $m_x := n_x/N$ of the total number N of particles. Therefore, one also can define reduced moments M'_k , which do not include the largest cluster. In figure 4 (left) the growth of the clusters can be seen concerning the first moment. After several collisions, the particles start to cluster and the moments of the cluster size distribution grow until they reach a saturation value (with huge fluctuations). A numerical analysis reveals that the increase in M_1 (and M_2) is mainly due to one large cluster which grows until it reaches its maximum size. In this final state this cluster contains a macroscopic fraction m_x of the particles, see figure 4 (right).

The onset time of cluster growth and also the final size m_x of the large cluster depend strongly on the restitution coefficient r (see figure 4 and [8]). At low dissipation rates, for a long time nothing interesting happens and finally small and strongly fluctuating clusters appear. High dissipation leads to almost immediate cluster growth and a very large cluster at last. On the other hand, the system size N does not seem to affect the behavior of the system provided that N is not too small (see [8]).

3.4 Cluster structure

In figure 5, zooms into the bottom-right area of the the same system as in figure 3 are presented in the late cluster growth and saturation regime. Here the clusters are very large and one obtains crystalline, triangular lattice structures with a peculiar distribution of collision rates as color-coded.

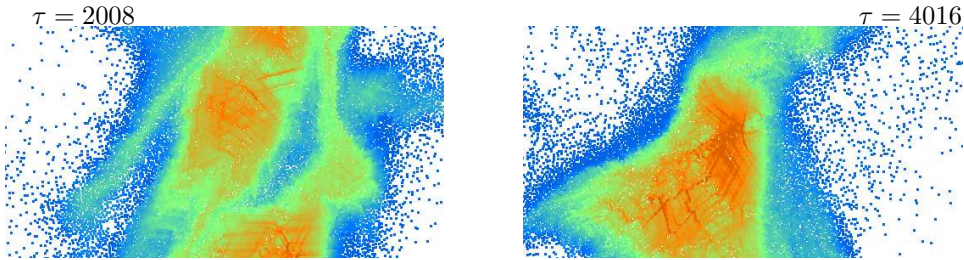


Figure 5. Zooms into the lower right part of the ED simulation from figure 3.

4. Summary

The evolution of freely cooling granular systems can be divided into three regimes: First, the system is in the homogeneous cooling state (HCS). The decay of the kinetic energy and the collision frequency can be described by simple analytical expressions $E(\tau) \sim (1 + \tau)^{-2}$ and $f_c(\tau) \sim (1 + \tau)^{-1}$. The time-scale is mainly determined by the density and the dissipation of the system.

After a few collisions per particle, clusters begin to develop and grow and the collision frequency, which can show large fluctuations because of cluster-cluster collisions, cannot be predicted anymore. The energy decay is characterized by $E \sim \tau^{-1}$. This regime shows interesting differences between two and three dimensions (see [8,25]).

After many more collisions, the clusters merge to one large cluster which grows until it reaches system size. Then the system behavior is dominated by one large cluster which contains a macroscopic fraction of the particles in the system. Kinetic energy and collision frequency still fluctuate, but are governed by the equations $E(\tau) \sim \tau^{-2}$ and $f_c(\tau) \sim \tau^{-1}$. This means the evolution in time is similar to the homogeneous cooling state.

Inside the clusters, density can grow above the crystallization limit (that happens frequently in 2D but was observed rarely in the 3D systems examined until now). We referred to the necessary corrections concerning the collision rate (which enters stress and dissipation rate and also the other transport coefficients).

In brief, due to crystallization the collision rate can be decreased relative to a disordered, fluid system, due to more efficient space filling. A strong increase in density – but not necessarily related to crystallization – makes multi-particle contacts possible. The control parameter is the ratio of the contact duration and the time between collisions. If the collision rate becomes larger than the inverse contact duration, dissipation is reduced, as compared to a hard sphere model with vanishing contact duration. An analytical expression for 3D systems was given, which corrects the dissipation rate in the multiple collision regime.

Acknowledgments

The author thanks A Goldshtein and S Miller for their cooperation on parts of these results and Hans Herrmann and Sean McNamara for helpful discussions. This

research was supported by the Deutsche Forschungsgemeinschaft (DFG) and FOM (Stichting Fundamenteel Onderzoek der Materie, The Netherlands) as financially supported by NWO (Nederlandse Organisatie voor Wetenschappelijk Onderzoek).

References

- [1] H J Herrmann, J-P Hovi and S Luding (eds) *Physics of dry granular media – NATO ASI Series E 350* (Kluwer Academic Publishers, Dordrecht, 1998)
- [2] T Pöschel and S Luding (eds) *Granular gases*, Lecture Notes in Physics 564 (Springer, Berlin, 2001)
- [3] P A Vermeer, S Diebels, W Ehlers, H J Herrmann, S Luding and E Ramm (eds) *Continuous and discontinuous modelling of cohesive frictional materials*, Lecture Notes in Physics 568 (Springer, Berlin, 2001)
- [4] Y Kishino (ed.) *Powders and Grains 2001* (Balkema, Rotterdam, 2001)
- [5] I Goldhirsch and G Zanetti, *Phys. Rev. Lett.* **70**(11), 1619 (1993)
- [6] S Luding and H J Herrmann, *Chaos* **9**(3), 673 (1999)
- [7] X Nie, E Ben-Naim and S Chen, *Phys. Rev. Lett.* **89**(20), 204301 (2002)
- [8] S Miller and S Luding, *Phys. Rev.* **E69**, 031305 (2004)
- [9] N V Brilliantov, C Saluena, T Schwager and T Pöschel, *Phys. Rev. Lett.* **93**(13), 134301 (2004)
- [10] I Goldhirsch, M-L Tan and G Zanetti, *J. Sci. Comput.* **8**, 1 (1993)
- [11] S McNamara and W R Young, *Phys. Rev.* **E53**(5), 5089 (1996)
- [12] R Brito and M H Ernst, *Europhys. Lett.* **43**(15), 497 (1998); cond-mat/9807224
- [13] S A Hill and G F Mazenko, *Phys. Rev.* **E67**, 061302 (2003)
- [14] B D Lubachevsky, *J. Comp. Phys.* **94**(2), 255 (1991)
- [15] S Miller and S Luding, *J. Comp. Phys.* **193**(1), 306 (2004)
- [16] M P Allen and D J Tildesley, *Computer simulation of liquids* (Oxford University Press, Oxford, 1987)
- [17] B D Lubachevsky, *Int. J. Computer Simulation* **2**, 373 (1992)
- [18] P K Haff, *J. Fluid Mech.* **134**, 401 (1983)
- [19] J T Jenkins and M W Richman, *Phys. Fluids* **28**, 3485 (1985)
- [20] S Luding and S McNamara, *Granular Matter* **1**(3), 113 (1998); cond-mat/9810009
- [21] S Luding and A Goldshtein, *Granular Matter* **5**(3), 159 (2003)
- [22] S Luding, M Huthmann, S McNamara and A Zippelius, *Phys. Rev.* **E58**, 3416 (1998)
- [23] S Luding, *Phys. Rev.* **E63**, 042201–1–4 (2001)
- [24] S Luding, *Adv. Complex Systems* **4**(4), 379 (2002)
- [25] S Miller, *Clusterbildung in granularen Gasen*, PhD thesis (Universität Stuttgart, 2004)
- [26] S Luding, E Clément, J Rajchenbach and J Duran, *Europhys. Lett.* **36**(4), 247 (1996)
- [27] S Luding, Surface waves and pattern formation in vibrated granular media, in: *Powders and Grains 97* (Balkema, Amsterdam, 1997) pp. 373–376
- [28] S Luding, E Clément, A Blumen, J Rajchenbach and J Duran, *Phys. Rev.* **E50**, 4113 (1994)
- [29] S Luding, Molecular dynamics simulations of granular materials, in: H Hinrichsen and D E Wolf (eds) *The physics of granular media* (Wiley VCH, Weinheim, Germany, 2004) pp. 299–324